Langmuir

Research Article

Approximate Analytical Expressions for the Electrical Potential in a Cavity Containing Salt-Free Medium

Shiojenn TsengNing-Bew WongPen-Chun Liu, and Jyh-Ping Hsu

Langmuir, **2007**, 23 (21), 10448-10454 • DOI: 10.1021/la7017456

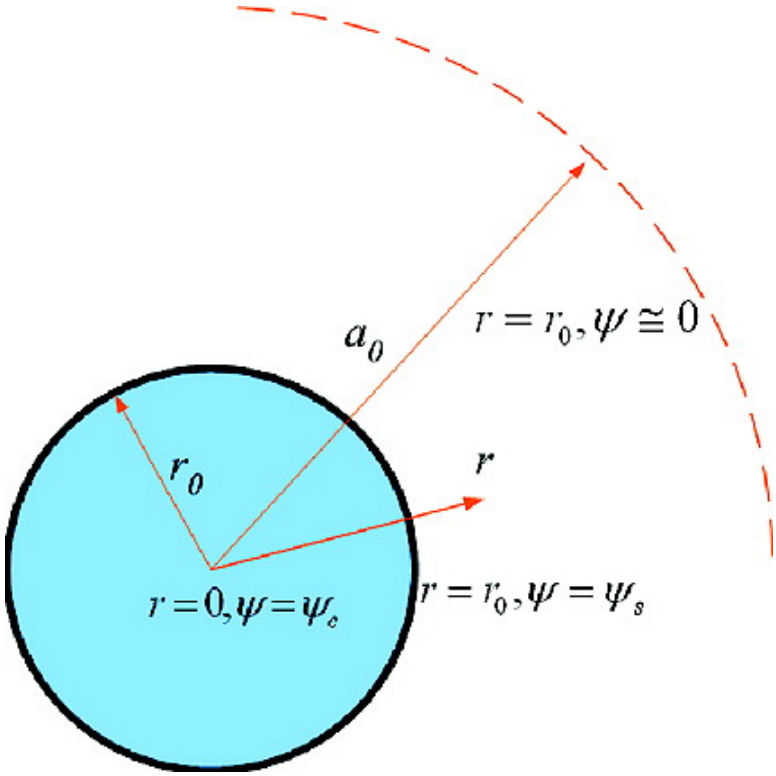

More About This Article

Additional resources and features associated with this article are available within the HTML version:

- Supporting Information
- Access to high resolution figures
- Links to articles and content related to this article
- Copyright permission to reproduce figures and/or text from this article

Articles

Approximate Analytical Expressions for the Electrical Potential in a Cavity Containing Salt-Free Medium

Shiojenn Tseng

Department of Mathematics, Tamkang University, Tamsui, Taipei, Taiwan 25137

Ning-Bew Wong

Department of Biology and Chemistry, City University of Hong Kong, Kowloon, Hong Kong

Pen-Chun Liu and Jyh-Ping Hsu*

Department of Chemical Engineering, National Taiwan University, Taipei, Taiwan 10617

Received June 13, 2007. In Final Form: July 30, 2007

The electrical potential in a closed surface such as a cavity containing counterions only is derived for the cases of constant surface potential and constant surface charge density. The results obtained have applications in, for example, microemulsion-related systems in which ionic surfactants are introduced to maintain the stability of a dispersion and electroosmotic flow-related analysis. An analytical expression for the electrical potential is derived for a planar slit, and the methodology used is modified to derive approximate analytical expressions for spherical and cylindrical cavities. The higher the surface potential, the better the performance of these expressions. For the case where the surface potential is above ca. 50 mV, the performance of the approximate analytical expressions can further be improved by multiplying a correction function.

Introduction

A dispersed system in which the ionic species in the dispersion medium come mainly from the dissociation of the functional groups carried by the dispersed phase is called a salt-free dispersion. Typical example in practice includes a reverse micelle system where ionic surfactants are introduced to maintain its stability. In this case, counterions are released to the liquid medium inside a reverse micelle and its inner surface becomes charged, the conditions of which are key to the determination of its structure and thermodynamic properties. Dispersions containing natural polyelectrolytes such as DNA, RNA, filamentous actin, and microtubules and synthetic polyelectrolytes such as poly(acrylic acid) can also be salt-free.

Knowledge about the electrical potential distribution near a charged colloidal entity is essential to the determination of the basic properties of the corresponding dispersion. Under appropriate conditions, this distribution is described by a Poisson−Boltzmann equation.[1] In general, solving this equation analytically is nontrivial even for a simple geometry. The only reported exact analytical result is that for an infinite planar surface in a symmetric electrolyte solution under the conditions of constant surface potential. Other than this case, a Poisson−Boltzmann equation needs to be solved either numerically or semianalytically. Many attempts have been made in the past to derive an approximate solution to a Poisson−Boltzmann equation for surfaces of various types and geometries under various conditions.[2−11]

For a salt-free dispersion, although the corresponding Poisson−Boltzmann equation becomes simpler because only counterions are present in the liquid phase, deriving an exact analytical solution is still nontrivial. Ohshima[12] was able to obtain a surface charge density−surface potential relationship for a spherical colloidal particle, the potential near a charged spherical colloidal particle,[13] and the potential around a polyelectrolyte-coated spherical particle.[14] Alfrey et al.[15] discussed the counterion distribution in solutions of rod-shaped polyelectrolytes. Taking the effect of ionic size into account, Hsu et al.[16] derived the distribution of ionic species in a reverse micelle and solved the electrical potential in planar, cylindrical, and spherical reverse micelles based on a series expansion approach.[17]

* Corresponding author. Tel: 886-2-23637448. Fax: 886-2-23623040. E-mail: jphsu@ntu.edu.tw.

(1) Hunter, R. J. *Foundations of Colloid Science*; Oxford University Press: New York, 2001.
(2) Hsu, J. P.; Kuo, Y. C. *J. Colloid Interface Sci.* **1994**, *167*, 35.
(3) Sader, J. E.; Lenhoff, A. M. *J. Colloid Interface Sci.* **1998**, *201*, 233.
(4) Hsu, J. P.; Liu, B. T. *J. Colloid Interface Sci.* **1999**, *217*, 219.
(5) Zholkovskij, E. K.; Dukhin, S. S.; Mishchuk, N. A.; Masliyah, J. H.; Czarnecki, J. *Colloids Surf. A* **2001**, *192*, 235.
(6) Chen, Z.; Singh, R. K. *J. Colloid Interface Sci.* **2002**, *245*, 301.
(7) López-García, J. J.; Horno, J.; Grosse, C. *J. Colloid Interface Sci.* **2002**, *251*, 85.
(8) Oyanader, M.; Arce, P. *J. Colloid Interface Sci.* **2005**, *284*, 315.
(9) Luo, G.; Liu, C.; Wang, H. P.; Hou, C.; Jin, J. *J. Dispersion Sci. Technol.* **2005**, *26*, 173.
(10) Tuinier, R. *J. Colloid Interface Sci.* **2003**, *258*, 45.
(11) Lin, S. H.; Hsu, J. P.; Tseng, S.; Chen, C. J. *J. Colloid Interface Sci.* **2005**, *281*, 255.
(12) Ohshima, H. *J. Colloid Interface Sci.* **2002**, *247*, 18.
(13) Ohshima, H. *J. Colloid Polym. Sci.* **2004**, *282*, 1185.
(14) Ohshima, H. *J. Colloid Interface Sci.* **2003**, *268*, 429.
(15) Alfrey, T.; Berg, P. W.; Morawetz, H. *J. Polym. Sci.* **1951**, *7*, 543.
(16) Hsu, J. P.; Jiang, J. M.; Tseng, S. *J. Phys. Chem. B* **2003**, *107*, 14429.
(17) Hsu, J. P.; Tseng, S.; Jiang, J. M. *J. Phys. Chem. B* **2005**, *109*, 8180.

10.1021/la7017456 CCC: $37.00
Published on Web 09/14/2007

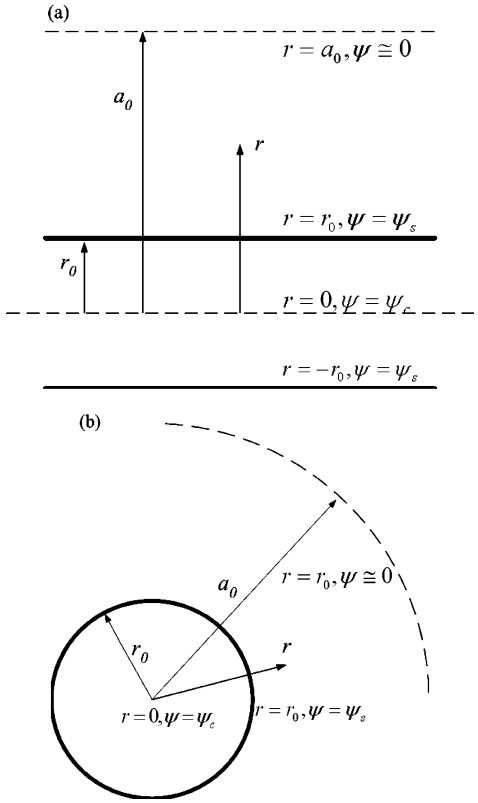

Figure 1. Schematic representation of the problem considered. (a) A planar slit of width $2r_0$, where r is the distance from the midplane of the slit. (b) A cylindrical or a spherical cavity of radius r_0, where r is the distance from the center of a cavity. In both (a) and (b), the electrical potential becomes negligible at $r = a_0$.

In a recent study, Hsu et al.[18] showed that the electrical potential between two spheres and that between two cylinders can be derived from the result of two parallel planes. In this study, their methodology is adopted to derive the electrical potential in a cavity containing salt-free medium only. The geometry under consideration includes a planar slit, a spherical cavity, and a cylindrical cavity. Both the case of constant surface potential and that of constant surface charge density are considered. The result obtained in this study has potential usage, for example, in the prediction and/or interpretation of several specific behaviors, such as clustering and electrical percolation, of lipid-stabilized water-in-oil microemulsions,[19−23] where the electrical interactions between dispersed liquid entities is believed to play an important role.[24−25] The results derived in this study are also applicable to the modeling of the electroosmotic flow in a microchannel containing salt-free solutions.

Theory

Referring to Figure 1, the geometry under consideration includes a planar slit, a spherical cavity, and a cylindrical cavity. Let $2r_0$ and r_0 be the width of a planar slit and the radius of a spherical or a cylindrical cavity, respectively. For a planar slit, r is the distance from the middle plane of a planar slit, and for a cylindrical and spherical surfaces, it is the radial distance from the center of a sphere or a cylinder. Let a_0 be the distance at which the electrical potential ψ becomes negligibly small. The liquid phase is salt-free, that is, the mobile ionic species (counterions) inside come mainly from that dissociated from the functional groups on a surface. Let b be the absolute value of the valence of counterions, C_b^0 be its molar concentration, and ϵ be the permittivity of the liquid phase. Suppose that ψ can be described by the Poisson−Boltzmann equation[18]

$$\frac{d^2\psi(r)}{dr^2} + \frac{\omega}{r}\frac{d\psi(r)}{dr} = \frac{bFC_b^0}{\epsilon}\exp\left[\frac{bF\psi(r)}{RT}\right] \quad (1)$$

Here, ω is a shape factor (= 0, 1, and 2 for planar, cylindrical, and spherical surfaces, respectively). F, R, and T are the Faraday constant, the gas constant, and the absolute temperature, respectively. For convenience, we define the scaled electrical potential $y = F\psi/RT$ and the scaled distance $x = \kappa r - \theta\kappa a_0 = \kappa r - \theta a$, where $a = \kappa a_0$, $\kappa = (2IF^2/\epsilon RT)^{1/2}$ is the Debye-Hückel parameter, and $I = C_b^0 b^2/2$ is the ionic strength. The geometry parameter θ is 0 for a planar slit and is 1 for both cylindrical and spherical cavities. In terms of the scaled symbols, eq 1 becomes

$$\frac{d^2y}{dx^2} + \frac{\omega}{x + a}\frac{dy}{dx} = \frac{1}{b}e^{by} \quad (2)$$

Constant Surface Potential. Consider first the case where the surface potential is maintained at a constant level. Then the boundary conditions associated with eq 2 can be expressed as

$$y = y_s \quad \text{at } x = d - a \quad (3)$$

$$y = y_c \quad \text{at } x = -a \quad (4)$$

where $d = \kappa r_0$, $y_s = F\psi_s/RT$, $y_c = F\psi_c/RT$, ψ_s is the surface potential, and ψ_c is the electrical potential on the middle plane of a planar slit or that on the center of a cylindrical or spherical cavity.

Following the treatment of Hsu et al.,[18] we consider first the case of a planar slit, that is, $\omega = 0$. It can be shown (Appendix) that the solution to eq 2 subject to eqs 3 and 4 is

$$y_{planar} = \frac{1}{b}\ln\left[\sec^2\left(\frac{\sqrt{2}}{2}(x + a)e^{by_{planar-c}/2}\right)\right] + y_{planar-c} \quad (5)$$

where y_{planar} is the scaled electrical potential for the case of a planar slit and $y_{planar-c}$ is the value of y_{planar} on the mid-plane of the planar slit which needs to be determined by (Appendix)

$$\tan^{-1}(\sqrt{e^{by_s - by_{planar-c}} - 1}) = \frac{\sqrt{2}\,r}{2}e^{by_{planar-c}/2} \quad (6)$$

For a spherical surface, $\omega = 2$, and eq 2 can rewritten by defining $u = [2+(x/a)]y$ as

$$\frac{d^2u}{dx^2} = \frac{[2 + (x/a)]}{b}\exp\left[\frac{bu}{[2 + (x/a)]}\right] \quad (7)$$

If $x/a \cong -1$, that is, the distance at which the electrical potential is negligibly small is much larger than the radius of a spherical cavity, then $[2 + (x/a)] \cong 1$, and eq 7 can be approximated by

$$\frac{d^2u}{dx^2} = \frac{1}{b}e^{bu} \quad (8)$$

(18) Hsu, J. P.; Yu, S. Y.; Tseng, S. *J. Phys. Chem. B* **2006**, *110*, 25007.
(19) Bisceglia, M.; Acosta, E.; Kurlat, D.; Ginzberg, B. *Colloids Surf. A* **1996**, *108*, 137.
(20) Moran, P. D.; Bowmaker, G. A.; Cooney, R. P.; Bartlett, J. R.; Woolfrey, J. L. *Langmuir* **1995**, *11*, 738.
(21) Nitsch, W.; Plucinski, P. *J. Colloid Interface Sci.* **1990**, *136*, 338.
(22) Hun, C. *J. Colloid Interface Sci.* **1979**, *71*, 408.
(23) Ekwall, P.; Mandell, L.; Fontell, K. *J. Colloid Interface Sci.* **1970**, *33*, 215.
(24) Lemaire, B.; Bothorel, P.; Roux, D. *J. Phys. Chem.* **1983**, *87*, 1023.
(25) Alexandridis, P.; Holzwarth, J. F.; Hatton, T. A. *J. Phys. Chem.* **1995**, *99*, 8222.

The corresponding boundary conditions are

$$u = u_s \quad \text{at } x = d - a \tag{9}$$

$$u = u_c \quad \text{at } x = -a \tag{10}$$

Referring to the solution for a planar slit, the solution to eq 8 subject to eqs 9 and 10 is

$$u = \frac{1}{b}\ln\left[\sec^2\left(\frac{\sqrt{2}}{2}(x+a)e^{bu_c/2}\right)\right] + u_c \tag{11}$$

or in terms of the original scaled symbols as

$$y_{spherical} = \left[\frac{1}{(2 + x/a)}\right]\frac{1}{b}\ln\left[\sec^2\left(\frac{\sqrt{2}}{2}(x+a)e^{bu_c/2}\right)\right] + u_c \tag{12}$$

where $y_{spherical}$ is the scaled electrical potential for the case of a spherical cavity and u_c is the value of u at its center ($r = 0$). Note that in eq 6, if $\exp[b(y_s - y_c)] \gg 1$, then $\tan^{-1}[\exp[b(y_s - y_c)] - 1]^{1/2} \cong (\pi/2) - \exp[b(y_s - y_c)/2]$, and therefore, u_c can be approximated by

$$u_c = \frac{2}{b}\ln\left[\frac{\pi}{\sqrt{2}\,r + 2e^{(-b(2+x/a)y_s)/2}}\right] \tag{13}$$

For the case of a cylindrical cavity, $\omega = 1$, and if we define $\upsilon = y/K_0[a(2 + x/a)]e^{a(2+x/a)}$, then eq 2 becomes

$$K_0[a(2+x/a)]e^{a(2+x/a)}\frac{d^2\upsilon}{dx^2} + K_0[a(2+x/a)]\left\{\frac{1}{a(2+x/a)} - 2\frac{K_1[a(2+x/a)]}{K_0[a(2+x/a)]} + 2\right\}e^{a(2+x/a)}\frac{d\upsilon}{dx} + K_0[a(2+x/a)]\left\{\frac{1}{a(2+x/a)} - \left[2 + \frac{1}{a(2+x/a)}\right]\times \frac{K_1[a(2+x/a)]}{K_0[a(2+x/a)]} + 2\right\}e^{a(2+x/a)}\upsilon = \frac{1}{b}e^{K_0[a(2+x/a)]e^{a(2+x/a)}b\upsilon} \tag{14}$$

where K_0 is the zeroth-order modified Bessel function of the second kind, and K_1 is the first-order modified Bessel function of the second kind. If $x/a \cong -1$ and $a \gg 1$, since $\{K_1[a(2 + x/a)]/K_0[a(2 + x/a)]\} \rightarrow 1$ and $[1/a(2 + x/a)] \rightarrow 0$, eq 14 can be approximated by

$$\frac{d^2[K_0(a)e^a\upsilon]}{dx^2} = \frac{1}{b}e^{K_0(a)e^a b\upsilon} \tag{15}$$

The corresponding boundary conditions are

$$K_0(a)e^a\upsilon = K_0(a)e^a\upsilon_s = y_s \quad \text{at } x = d - a \tag{16}$$

$$K_0(a)e^a\upsilon = K_0(a)e^a\upsilon_c = y_c \quad \text{at } x = -a \tag{17}$$

Referring to the solution for a planar slit, the solution to eq 15 subject to eqs 16 and 17 is

$$K_0(a)e^a\upsilon = \frac{1}{b}\ln\left[\sec^2\left(\frac{\sqrt{2}}{2}(x+a)e^{b\upsilon_c/2}\right)\right] + \upsilon_c \tag{18}$$

In terms of the original scaled symbols, we have

$$y_{cylindrical} = \frac{K_1[a(2+x/a)]e^{a(2+x/a)}}{K_0(a)e^a}\frac{1}{b}\ln\left[\sec^2\left(\frac{\sqrt{2}}{2}(x+a)e^{b\upsilon_c/2}\right)\right] + \upsilon_c \tag{19}$$

where $y_{cylindrical}$ is the scaled electrical potential for the case of a cylindrical cavity and υ_c is the value of υ at its center ($r = 0$). Applying the condition that for $\exp[b(y_s - y_c)] \gg 1$, $\tan^{-1}[\exp[b(y_s - y_c)] - 1]^{1/2} \cong (\pi/2) - \exp[b(y_s - y_c)/2]$, it can be shown that

$$\upsilon_c = \frac{2}{b}\ln\left\{\frac{\pi}{\sqrt{2}r + 2\exp\dfrac{-b[K_0(a)e^a(y_s/K_0[a(2+x/a)])]e^a(2+x/a)}{2}}\right\} \tag{20}$$

Constant Surface Charge Density. Let us consider next the case in which the surface of a cavity is maintained at a constant charge density. In a micelle, for example, the surface charge arises from the dissociation of the functional groups on a surfactant layer. In this case, the boundary condition for the electrical potential can be expressed as[1,17]

$$\frac{dy}{dx} = \frac{-b^2e^2\gamma\rho X_s}{\epsilon kT} = \sigma \quad \text{at } x = d - a \tag{21}$$

where ρ is the surface density of dissociable functional groups, X_s is the mole fraction of dissociated functional groups, γ is the effective interaction energy per molecule arising from headgroup repulsion, and σ is the scaled surface charge density. Substituting eq 21 into eq A-4 yields

$$y_s = \frac{1}{b}\ln\left(\frac{1}{2}b^2\sigma^2\right) + y_c \tag{22}$$

Therefore, for a given value of σ, y_s is evaluated by this expression, and the same procedure used to evaluate the electrical potential for the case of constant surface potential can be followed.

Results and Discussion

Figures 2−4 illustrate the simulated spatial variations of the scaled electrical potential for a planar slit, a spherical cavity, and a cylindrical cavity, respectively. Both the exact numerical results and the results based on the present approach are presented. The former are obtained from IMSL,[26] which is based on a nonuniform-mesh finite difference method. The excellent agreement between the numerical result and the result based on eqs 5 and 6 is expected since the latter is exact for a planar slit. However, the performance of the approximate analytical expressions for a spherical cavity and that for a cylindrical cavity depend upon the level of the surface potential. In general, the higher the surface potential, the better the performance, and the deviation of the analytical expressions for a spherical cavity is larger than that for a cylindrical cavity. The former is because we assume $a \gg 1$ in the derivation of the electrical potential for a spherical and a cylindrical cavity, since the higher the level of y_s the larger the value of a, and therefore, the more appropriate the assumption $a \gg 1$. Note that although the present result for a planar slit, eqs 5 and 6, has a different appearance than that of Hsu et al.,[18] both are exact and lead to the same numerical value.

(26) IMSL, Compaq Visual Fortran, 6.6.0, Compaq Copmuter Co., U.S.A., 2001.

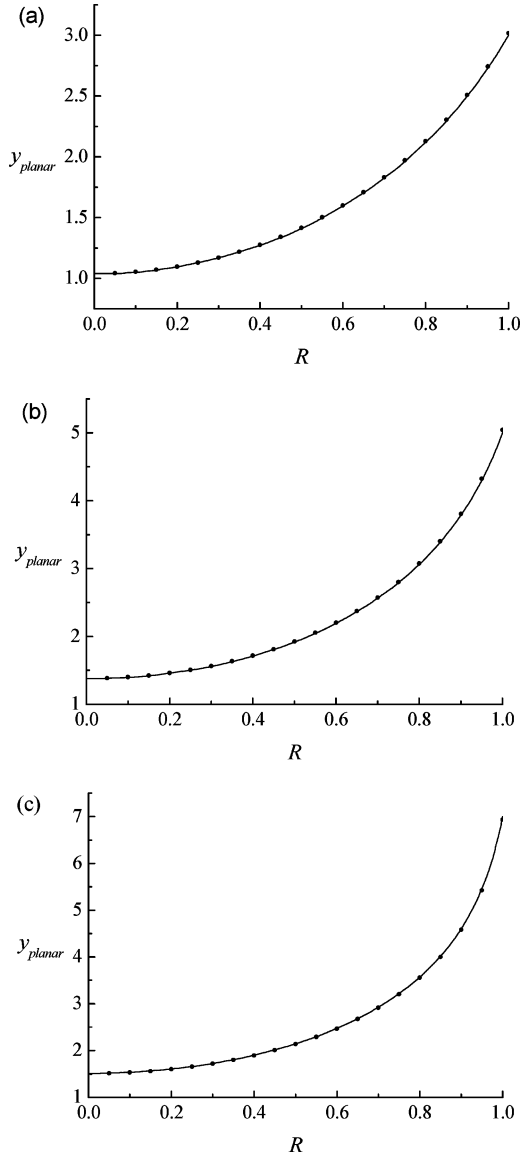

Figure 2. Spatial variation of the scaled electrical potential in a planr slit at various levels of scaled surface potential y_s, $R = (x + a)/\kappa r_0$ is the scaled distance. (a) $y_s = 3$, (b) $y_s = 5$, (c) $y_s = 7$. Curves: exact numerical results, discrete symbols: present results using eqs 5 and 6.

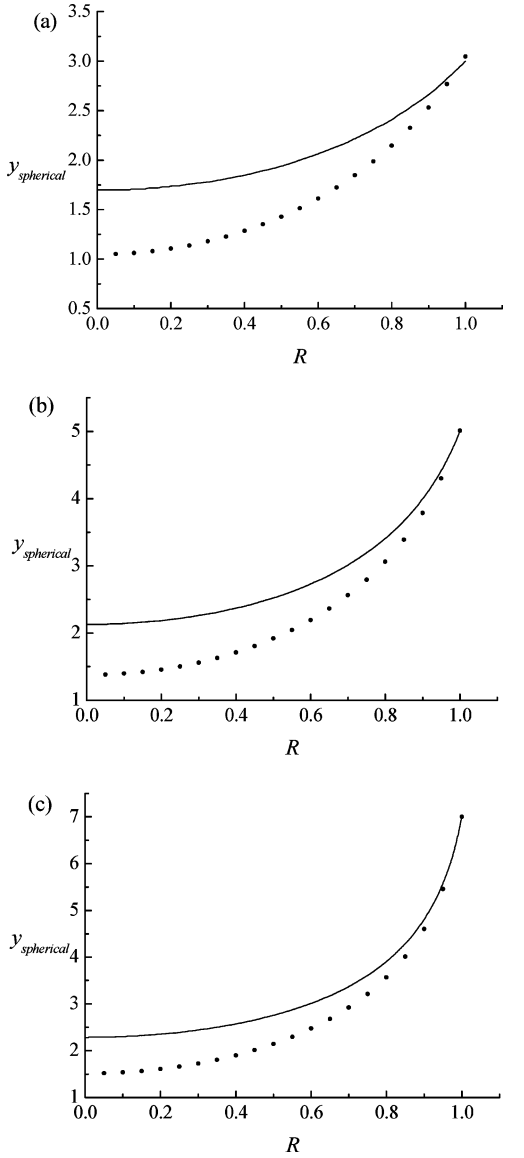

Figure 3. Spatial distribuitons of the scaled electrical potential in a spherical cavity for various combinaitons of y_s and b at $a = 1000$, $R = (x + a)/\kappa r_0$ is the scaled distance. (a) $y_s = 3$, (b) $y_s = 5$, (c) $y_s = 7$. Curves: exact numerical results; discrete symbols: approximate analytical expression based on eqs 12 and 13.

Figures 3 and 4 reveal that the maximum deviation of the approximate analytical expressions occurs at the center of a cavity. For example, if $y_s = 3$, the deviation is 38% for a spherical cavity and 25% for a cylindrical cavity. Also, the higher the surface potential, the smaller the deviation is. The large deviation at the center of a cavity arises mainly from using the approximate expression u_c for a spherical cavity, eq 13, and υ_c for a cylindrical cavity, eq 20. The performance of the approximate analytical expression for a spherical cavity and that for a cylindrical cavity can be improved by multiplying a correction function as below

$$y_{\text{spherical}} = F_{\text{spherical}}\left[\frac{1}{(2 + x/a)}\right]\frac{1}{b}\ln\left[\sec^2\left(\frac{\sqrt{2}}{2}(x + a)e^{bu_c/2}\right)\right] + u_c \quad (23)$$

$$F_{\text{spherical}} = (0.05y_s - 0.88)(R) + (-0.04y_s + 1.83), \quad 2 \le y_s \quad (24)$$

where $R = (x + a)/\kappa r_0$. The coefficients in the correction functions F_{sphrical} and $F_{\text{cylindrical}}$ are estimated through a regression analysis. First, for each $y_s = 1, 2, ..., 6$, the exact numerical values of $y_{\text{spherical}}(R)$ and $y_{\text{cylindrical}}(R)$ at 50 mesh points generated by IMSL for R in the range [0,1] are obtained. Then, the coefficients of F_{sphrical} in eq 24 are chosen based on the minimum sum of square difference, $\sum_{i=1}^{50}[y_{\text{spherical}}(R_i)$ using eq 12; $y_{\text{spherical}}(R_i)$ using eq 23].[2] The coefficients in the correction functions $F_{\text{cylindrical}}$ are estimated in a similar way. Figure 5 shows the simulated spatial variations of the scaled electrical potential based on these expressions. This figure reveals that the performance of the approximate analytical expression, eqs 12 and 19, can be improved appreciably by using the modified approximate analytical expressions, eqs 23−26. For example, if $y_s = 3$, the deviation at the center of a spherical cavity reduces to 3.4% and to 2% for a cylindrical cavity. Equations 23−26 are applicable for $2 \le y_s$, that is, the surface potential exceed ca. 50 mV. If the surface potential is low, eq 1 can be solved directly.

In the derivation of the electrical potential for spherical and

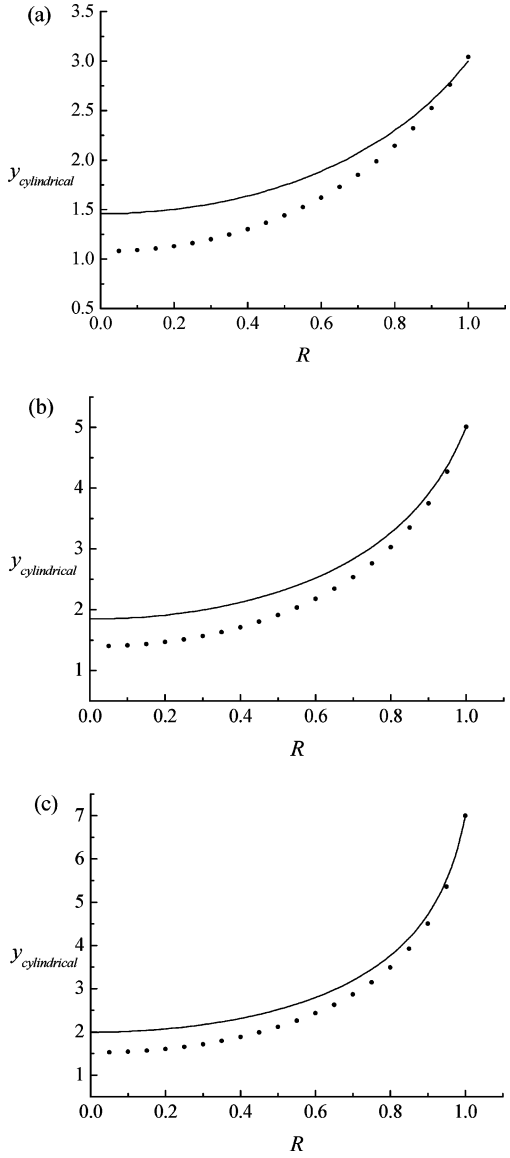

Figure 4. Spatial distribuitons of the scaled electrical potential in a cylindrical cavity for various combinaitons of y_s and b at $a = 700$, $R = (x + a)/\kappa r_0$ is the scaled distance. (a) $y_s = 3$, (b) $y_s = 5$, (c) $y_s = 7$. Curves: exact numerical results; discrete symbols: approximate analytical expression based on eqs 19 and 20.

$$y_{\text{cylindrical}} = F_{\text{cylindrical}} \frac{K_1[a(2 + x/a)]e^{a(2+x/a)}}{K_0(a)e^a} \times \frac{1}{b} \ln\left[\sec^2\left(\frac{\sqrt{2}}{2}(x + a)e^{b\upsilon_c/2}\right)\right] + \upsilon_c \quad (25)$$

$$F_{\text{cylidrincal}} = (0.04y_s - 0.58)(R) + (-0.03y_s + 1.53), \quad 2 \le y_s \quad (26)$$

cylindrical cavities, a length scale a is defined where the electrical potential can be neglected if the scaled distance from the center of a cavity exceeds a. To examine the order of magnitude of a, an overall percentage deviation Er_s is defined for the case of a spherical cavity as

$$Er_s = \frac{\int_0^1 |y_{s,n} - y_{s,a}|\, dx}{\int_0^1 |y_{s,n}|\, dx} \times 100\% \quad (27)$$

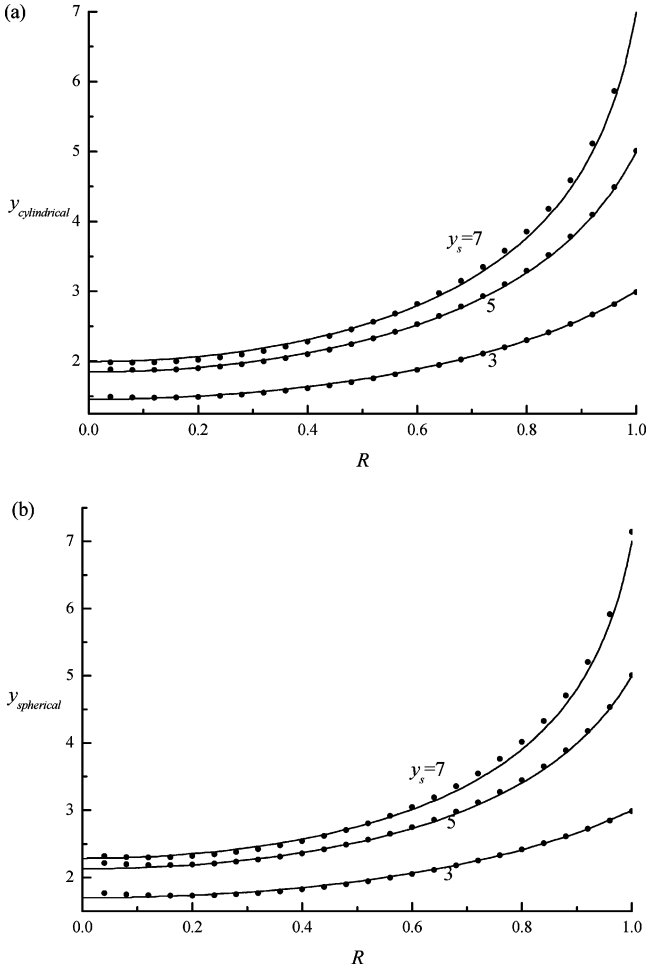

Figure 5. Spatial distribuitons of the scaled electrical potential in a cylindrical cavity $y_{\text{cylindrical}}$, (a), and a spherical cavity $y_{\text{spherical}}$, (b), for various levels of y_s at $b = 1$ and $a = 1000$, $R = (x + a)/\kappa r_0$ is the scaled distance. Curves: exact numerical results; discrete symbols: modified approximate analytical expressions, eqs 13 and 24 for a cylindrical cavity, and eqs 20 and 26 for a spherical cavity.

where $y_{s,n}$ and $y_{s,a}$ are respectively the scaled electrical potential for a spherical surface based on the numerical solution of eq 2 and that based on the approximate expressions, eqs 12 and 13. Similarly, for a cylindrical cavity, we define an overall percentage deviation Er_c as

$$Er_c = \frac{\int_0^1 |y_{c,n} - y_{c,a}|\, dx}{\int_0^1 |y_{c,n}|\, dx} \times 100\% \quad (28)$$

where $y_{c,n}$ and $y_{c,a}$ are the scaled electrical potential for a cylindrical surface based on the numerical solution of eq 2 and that based on the approximate expressions, eqs 19 and 20, respectively. Figure 6 reveals that a is on the order of 1000 for a spherical cavity and 700 for a cylindrical cavity.

The influence of the geometry of a cavity on the spatial distribution of the scaled electrical potential y is illustrated in Figure 7. This figure indicates that for a fixed surface potential, the rate of decreases in y as x declines for various geometries ranks as follows: planar slit < cylindrical cavity < spherical cavity, which is consistent with the result of Hsu et al.[18] for the electrical potential between two planes, two spheres, and two cylinders and can be explained by the same reasoning.

Figure 8 shows the influence of the valence of counterions b on the spatial distribution of the scaled electrical potential in a

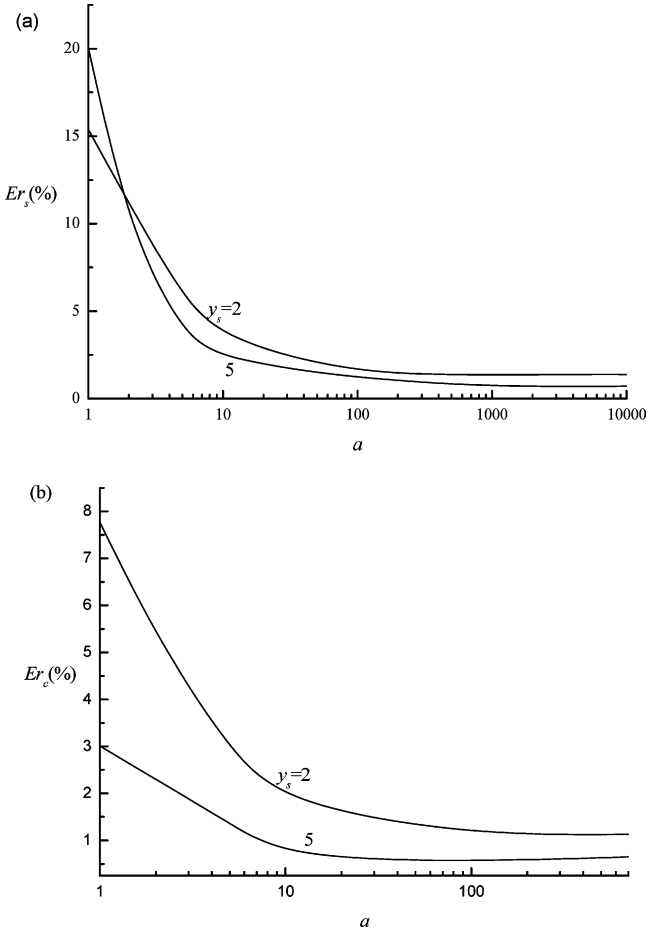

Figure 6. Variations of the overall percentage deviation for a spherical cavity Er_s, (a), and a cylindrical cavity Er_c (b), as a function of a, for two levels of y_s at $b = 1$.

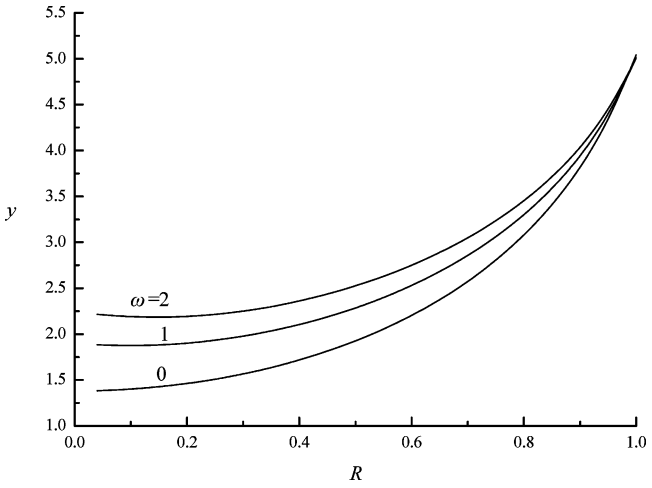

Figure 7. Spatial distribuitons of the scaled electrical potential y for various types of cavity at $y_s = 5$ and $b = 1$, $R = (x + a)/\kappa r_0$ is the scaled distance. The values of ω are 0, 1, and 2 for planar slit, cylindrical cavity, and spherical cavity, respectively.

spherical cavity at various levels of the scaled surface potential y_s. This figure reveals that the smaller the b the higher the $y_{spherical}$ and the slower the rate of decay of $y_{spherical}$ as x declines. Also, the smaller the b the more accurate the modified approximate analytical result, eqs 13 and 23. These arise from that for a fixed cavity size; the larger the b, the higher the ionic strength, and the thinner the double layer, the smaller the a and, therefore, the more inappropriate the assumption of $a \gg 1$. The behaviors of

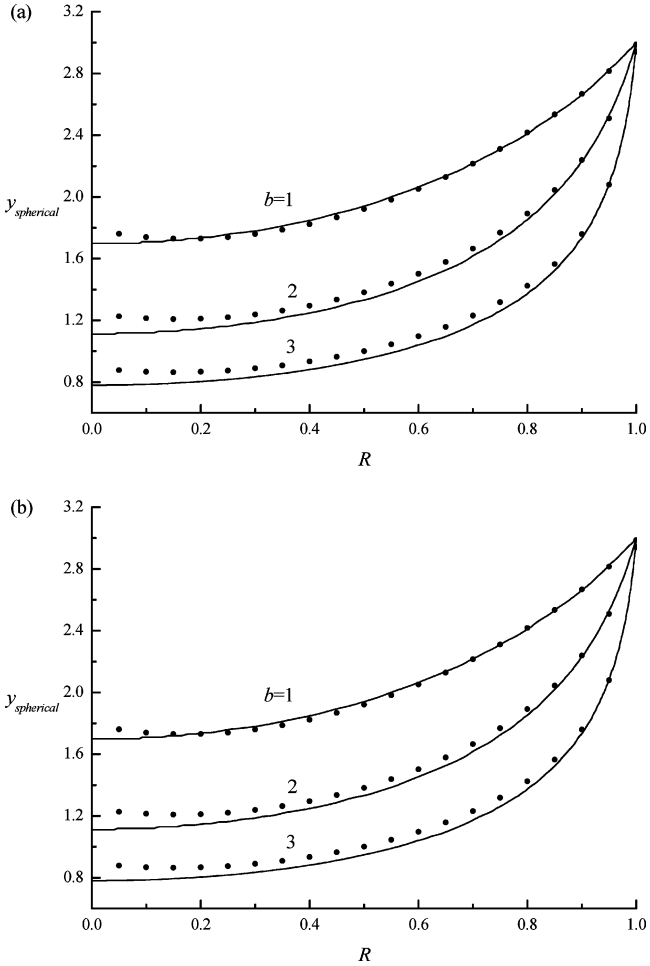

Figure 8. Spatial distributions of the scaled electrical potential in a spherical cavity for various combinations of y_s and b at $a = 1000$, $R = (x + a)/\kappa r_0$ is the scaled distance. (a) $y_s = 2$, (b) $y_s = 3$. Curves: exact numerical results; discrete symbols: approximate analytical expression based on eqs 13 and 23.

$y_{cylindrical}$ as x varies are similar to those observed in Figure 8 for a spherical cavity.

Conclusions

The electrical potential in a planar slit is derived analytically and the same methodology used to derive an approximate expression for the electrical potential in a spherical cavity and in a cylindrical cavity. The results obtained have practical applications, for example, in the evaluation of the properties of an emulsion system in which knowing the electrical potential inside a micelle is necessary. The performance of the approximate expression for the electrical potential in a spherical cavity and that in a cylindrical cavity is satisfactory if the surface potential is sufficiently high. If this is not the case, the performance can be improved appreciably by multiplying a correction function, which depends on the level of the surface potential and the radius of a cavity. The present analysis is applicable to both the case of constant surface potential and that of constant surface charge density.

Appendix

For a planar slit, $\omega = 0$, eq 2 becomes

$$\frac{d^2y}{dx^2} = \frac{1}{b} e^{by} \tag{A1}$$

Integrating once gives

$$\frac{dy}{dx} = \frac{\sqrt{2}}{b} \sqrt{e^{by} + C} \tag{A2}$$

where C is an integration constant. Applying the conditions

$$\frac{dy}{dx} = 0 \quad \text{and } y = y_{\text{planar-c}} \quad \text{at } x = -a \tag{A3}$$

C can be determined. Substituting the value of C thus obtained into eq A-2 yields

$$\frac{dy}{dx} = \frac{\sqrt{2}}{b} \sqrt{e^{by} + e^{by_{\text{planar-c}}}} \tag{A4}$$

Integrating this expression from $x = d - a$ and $y = y_s$ to $x = -d - a$ and $y = y_s$, we obtain

$$e^{by - by_{\text{planar-c}}} = \tan^2\left(\frac{\sqrt{2}}{2} e^{by_{\text{planar-c}}/2}(x + a)\right) + 1 \tag{A5}$$

Solving this expression for y gives the scaled electrical potential in a planar slit, y_{planar}

$$y_{\text{planar}} = \frac{1}{b} \ln\left[\sec^2\left(\frac{\sqrt{2}}{2}(x + a)e^{by_{\text{planar-c}}/2}\right)\right] + y_{\text{planar-c}} \tag{A6}$$

which is eq 5 in the text.

Integrating eq A-4 from the lower plane to the upper plane yields

$$\int_{y_s}^{y_s} \pm \frac{dy}{\sqrt{e^y - e^{y_{\text{planar-c}}}}} = \int_{-d-a}^{d-a} \frac{\sqrt{2}}{b} dx \tag{A7}$$

where $d = \kappa r_0$ is the scaled distance from the mid-plane of a planar slit. This expression can be rewritten aswhich becomes,

$$\int_{y_{\text{planar-c}}}^{y_s} \frac{dy}{\sqrt{e^y - e^{y_{\text{planar-c}}}}} - \int_{y_s}^{y_{\text{planar-c}}} \frac{dy}{\sqrt{e^y - e^{y_{\text{planar-c}}}}} = \frac{2\sqrt{2}}{b} d \tag{A8}$$

after performing the integration

$$\tan^{-1}\left(\sqrt{e^{by_s - by_{\text{planar-c}}} - 1}\right) = \frac{\sqrt{2}\, r}{2} e^{by_{\text{planar-c}}/2} \tag{A9}$$

This is eq 6 in the text. If $\exp[b(y_s - y_c)] \gg 1$, then $\tan^{-1}[\exp[b(y_s - y_c)] - 1]^{1/2} \cong (\pi/2) - \exp[b(y_s - y_c)/2]$, and eq A9 can be approximated as

$$y_{\text{planar-c}} = \frac{2}{b} \ln\left(\frac{\pi}{\sqrt{2}\, r + 2e^{-by_s/2}}\right) \tag{A10}$$

Acknowledgment. This work is supported by the National Science Council of the Republic of China.

LA7017456